Electromagnetic form factors of the nucleon: new fit and analysis of uncertainties

W. M. Alberico[1], S. M. Bilenky[2,3], C. Giunti[1], and K. M. Graczyk[1,4*]
[1] *Dipartimento di Fisica Teorica, Università di Torino and INFN, Sezione di Torino, I–10125 Torino, Italy*
[2] *BLTP, JINR, RU-141980 Dubna, Russia*
[3] *Physics-Department E15, Technische Universität München, D-85748 Garching, Germany and*
[4] *Institute of Theoretical Physics, University of Wrocław, pl. M. Borna 9, 50-204, Wrocław, Poland*
(Dated: June 8, 2009)

Electromagnetic form factors of proton and neutron, obtained from a new fit of data, are presented. The proton form factors are obtained from a simultaneous fit to the ratio $\mu_p G_{Ep}/G_{Mp}$ determined from polarization transfer measurements and to *ep* elastic cross section data. Phenomenological two-photon exchange corrections are taken into account. The present fit for proton was performed in the kinematical region $Q^2 \in (0, 6)$ GeV^2. Both for protons and neutrons we use the latest available data. For all form factors the uncertainties and correlations of form factor parameters are investigated with the χ^2 method.

PACS numbers: 13.40.Gp, 14.20.Dh, 13.60.Fz
Keywords: electromagnetic nucleon form factors, elastic electron-nucleon scattering, two photon exchange corrections

arXiv:0812.3539v2 [hep-ph] 8 Jun 2009

1. INTRODUCTION

The nucleon electromagnetic form factors are fundamental quantities, of great theoretical and experimental importance. The issue of their determination has been revisited in recent years, thanks to the results of several experiments at Bates, MAMI, JLab, which put under question previous analyses based on less precise data and urged the necessity for a new parameterization and a new analysis of the form factors themselves (for a review, see, for example Refs. [1, 2, 3]).

A precise knowledge of the electromagnetic form factors of the nucleon is important for the determination of the axial nucleon form factor in charged current (CC) quasielastic neutrino-nucleon scattering [4] and strange form factors of the nucleon in neutral current (NC) elastic neutrino-nucleon scattering. For example, NC vector form factors which characterize elastic NC scattering are given by the following expressions [5]:

$$G_E^{NC;p(n)} = \pm\frac{1}{2}\left\{G_{Ep} - G_{En}\right\} - 2\sin^2\theta_W G_{Ep(n)} - \frac{1}{2}G_{Es}$$
$$G_M^{NC;p(n)} = \pm\frac{1}{2}\left\{G_{Mp} - G_{Mn}\right\} - 2\sin^2\theta_W G_{Mp(n)} - \frac{1}{2}G_{Ms}\,.$$

In the above the dominant terms are the electric (G_E) and magnetic (G_M) form factors of the nucleon. Their precise knowledge is essential in order to determine the small strange form factors of the nucleon G_{Es}, G_{Ms}. Hence, it is obvious that not only a good knowledge of the electromagnetic form factors is required, but also the present level of their uncertainty.

In this paper we performed new fits of the nucleon electromagnetic form factors. The proton ones are extracted from: i) elastic *ep* cross section data, ii) polarization data, providing the $\mu_p G_E/G_M$ ratio (μ_p being the magnetic moment of the proton). The neutron form factors are extracted from electron-nucleus (typically deuterium and ^{3}He) scattering processes. The latest experimental data are used.

The proton form factors determined from the measurements of polarization transfer in elastic electron-proton scattering (first appearing between '99 and '02) were in a significant disagreement with respect to the ones obtained from elastic *ep* scattering data via the customary Rosenbluth separation. The main suggestion to solve this inconsistency was to account for two photon exchange (TPE) diagrams [6, 7, 8, 9], which should affect the cross section to a greater extent than the polarization data.

This disagreement became even more evident after the new JLab data on *ep* scattering cross sections [10] appeared. Hence, as already pointed out by several authors (see e.g. [11]), a reliable global fit must include the TPE correction;

*Electronic address: graczyk@to.infn.it

we will explicitly show the effect of TPE on the goodness of the fit (GoF). For a recent review devoted to TPE correction see Ref. [12].

There exist several parameterizations of the nucleon form factors which have been considered in the literature [11, 13, 14, 15, 16, 17, 18, 19, 20, 21, 22]. Among these, the older ones have a purely empirical Q^2 dependence [13, 14, 15, 16]:

$$G_{Ep}(Q^2), G_{Mp}(Q^2)/\mu_p \sim \frac{1}{1+\sum_{i=1}^{N} c_i Q^i}, \quad Q=\sqrt{Q^2}.$$

The specific form of the parameterization may depend on the Q^2 region. For instance, in Ref. [19] the low-Q^2 data were analyzed with form factors given by a continued fraction parameterization:

$$G_{Ep}(Q^2), G_{Mp}(Q^2)/\mu_p \sim \cfrac{1}{1+\cfrac{b_1 Q^2}{1+\cfrac{b_2 Q^2}{1+...}}}.$$

The newest empirical form factors are constrained to have a proper physical behavior at low-Q^2 as well as at high-Q^2. One of the examples is the Kelly's parameterization [18], which will be employed in our analysis (see next Section). The form factors depend on powers of the invariant Q^2, and for large Q^2 the form factors behave like $1/Q^4$. In Ref. [20] Kelly's parameterization is additionally constrained to satisfy duality hypothesis and the low-Q^2 behavior is described as in Ref. [19].

The electric neutron form factor, usually, is separately treated and described with a smaller number of parameters [23] (see also [24]).

It is also worth mentioning those parameterizations obtained on the basis of the vector meson dominance model. In particular the parameterization proposed by Lomon [22] seems especially suited to successfully describe the neutron form factor data.

In the present paper we aim to provide reliable fits of both proton and neutron e.m. form factors, by employing a relatively small number of parameters; moreover one of the major merits of this work is the analysis of errors on the parameters of the fit, which allows one to estimate the present uncertainty on our knowledge of the electromagnetic form factors.

The paper is organized as follows: in Section 2 we consider the proton form factors, by analyzing both the polarization data (Section 2.1) and the cross section data (Section 2.2). Section 3 is devoted to the neutron form factors, separately considering the electric and the magnetic form factors. Finally Section 4 presents a discussion of our results in comparison with previous analyses and the conclusions.

2. PROTON FORM FACTORS

In Section 2.1 we consider the recent polarization transfer and asymmetry measurements data which give an information on the ratio of the electric and magnetic proton form factors. Then, in Section 2.2, we present the results of the combined fit of the polarization and cross section data.

2.1. Fit of polarization data

In this section we consider the direct determination of the ratio of the electric and magnetic proton form factors

$$\mathcal{R}(Q^2) \equiv \mu_p \frac{G_{Ep}(Q^2)}{G_{Mp}(Q^2)}, \tag{1}$$

which has been obtained with the measurement of the polarization of the recoil proton and with asymmetry measurements. Here $Q^2 \equiv -q^2$, q being the four-momentum transfer. In the one-photon approximation q is the four-momentum of the virtual photon.

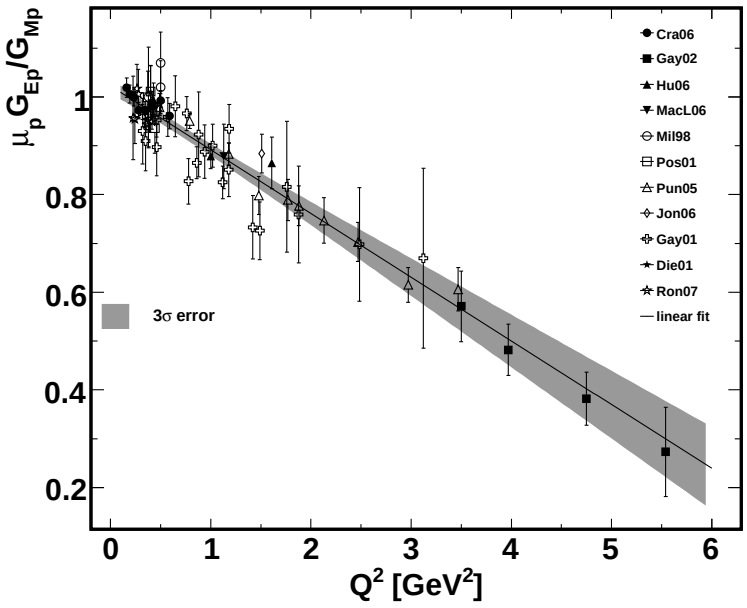

FIG. 1: Linear fit (9) of the recoil polarization and asymmetry measurements of the ratio $\mu_p G_{Ep}/G_{Mp}$. The shadowed area denotes the 3σ C.L. region of the fit.

The recoil polarization technique (see Ref. [3]) has been employed in several *ep* experiments for a direct measurement of the ratio $\mathcal{R}(Q^2)$. In the laboratory frame it is given by:

$$\mathcal{R}(Q^2) = -\mu_p \, \frac{P_t}{P_l} \, \frac{E+E'}{2M} \, \tan\!\left(\frac{\theta}{2}\right) , \tag{2}$$

where P_l and P_t are the longitudinal and transverse components of the polarization of the recoil proton, M is the proton mass, E and E' are the initial and final electron energies, and θ is the electron scattering angle. The latter is related to Q^2 according to:

$$Q^2 = 4EE' \sin^2\left(\frac{\theta}{2}\right) . \tag{3}$$

The ratio $\mathcal{R}(Q^2)$ has been also determined from the measurement of the asymmetry in elastic *ep* scattering with both polarized beam and target: we have (see Ref. [3])

$$\frac{\sigma_+ - \sigma_-}{\sigma_+ + \sigma_-} \;=\; -2\mu_p \sqrt{\tau(1+\tau)} \tan\!\left(\frac{\theta}{2}\right) \frac{\mathcal{R}\sin\theta^* \cos\phi^* + \mu_p \sqrt{\tau[1+(1+\tau)\tan^2\left(\frac{\theta}{2}\right)]}\cos\theta^*}{\mathcal{R}^2 + \mu_p \tau/\epsilon} , \tag{4}$$

where σ_+ and σ_- are the cross sections for positive and negative electron helicities, respectively, θ^* and ϕ^* are the polar and azimuthal angles of the target polarization relative to the three-momentum transfer vector $\vec{q}$ and the scattering plane (in the laboratory frame),

$$\tau \equiv \frac{Q^2}{4M^2} , \tag{5}$$

and

$$\epsilon \equiv \left[1 + 2(1+\tau)\tan^2\!\left(\frac{\theta}{2}\right)\right]^{-1} \tag{6}$$

is the virtual photon polarization.

We consider the recoil polarization and asymmetry data published in Refs. [25, 26, 27, 28, 29, 30, 31, 32, 33, 34, 35, 36]. These data are plotted in Fig. 1, together with their error bars, which include the statistical and systematic

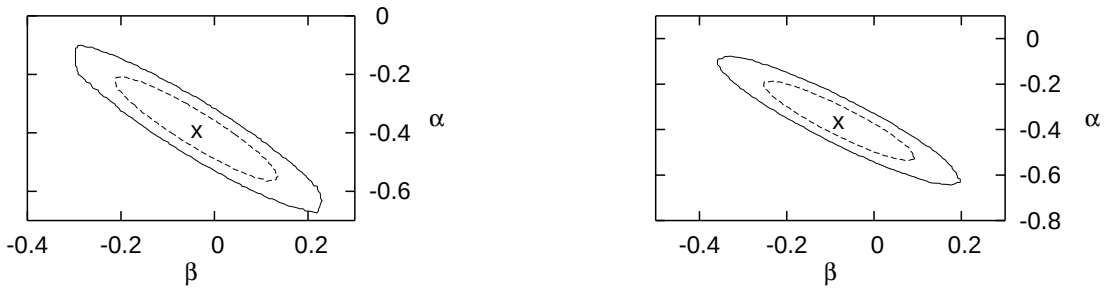

FIG. 2: Projection on the $\alpha - \beta$ parameter space of the contours delimiting the allowed regions in the 2-dimensional space of TPE correction parameters, with 1σ (dashed lines) and 2σ (solid lines) C.L. The contours are computed for fit I (left figure) and fit II right figure. The crosses indicate the projections of the best-fit point, Eq. (28) for fit I and Eq. (31) for fit II.

uncertainties added in quadrature. The Q^2 range of the data goes from 0.15 to 5.6 GeV^2. As one can see from Fig. 1, all data are well described by a linear function in Q^2:

$$\mathcal{R}(Q^2) = c_0 + c_1 Q^2. \tag{7}$$

We fitted the data points with this linear function, by minimizing the least-squares function

$$\chi^2_{\rm rat} = \sum_{j=1}^{N_{\rm rat}} \frac{(\mathcal{R}(Q^2_j) - \mathcal{R}^{\rm exp}_j)^2}{(\Delta\mathcal{R}^{\rm exp}_j)^2}. \tag{8}$$

where $N_{\rm rat} = 65$ is the total number of recoil polarization and asymmetry data points and $\mathcal{R}^{\rm exp}_j$ is the value of the ratio at the squared-momentum transfer Q^2_j, with corresponding uncertainty $\Delta\mathcal{R}^{\rm exp}_j$.

We found the following best fit values of the parameters:

$$c_0 = 1.022 \pm 0.005\,, \qquad c_1 = -0.130 \pm 0.005\,, \tag{9}$$

with 1σ uncertainties computed from the covariance matrix[1] (they are given by the square-roots of the diagonal elements of the covariance matrix).

The corresponding minimum χ^2 being:

$$(\chi^2_{\rm rat})_{\rm min}/{\rm NDF} = 58.89/63\,, \tag{10}$$

where NDF $= N_{\rm rat}$ is the number of degrees of freedom; the goodness of the fit (see Ref. [38]) is 62%.

The solid line in Fig. 1 corresponds to the best-fit values of the parameters in Eq. (9), while the shadowed area denotes 3σ C.L. region of the fit. One can see that the linear fit has small uncertainties, especially for $Q^2 \lesssim 3\,{\rm GeV}^2$, where there are many data points.

The best-fit values of the parameters c_0 and c_1 in Eq. (9) are close to those obtained by Arrington in Ref. [16], $c_0^{\rm bf} = 1.0324$ and $c_1^{\rm bf} = -0.135$. Let us notice that in Ref. [16] it was assumed that for $Q^2 < 0.24$ GeV^2 the form factor ratio is equal to one.

2.2. Fit of polarization and cross section data

The values of the proton form factors have been extracted from the data of many elastic ep scattering experiments using the Rosenbluth method. In the one-photon approximation, the differential cross section in the laboratory frame

[1] Detailed numbers of the covariance matrices relative to these and to the following fit parameters can be found in Ref. [37].

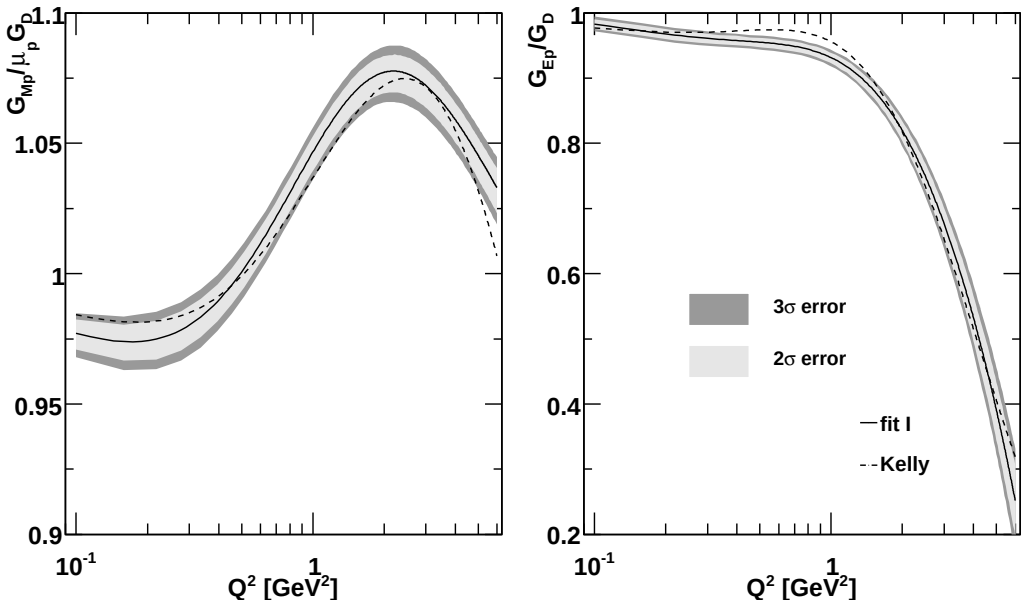

FIG. 3: The fits of $G_{Mp}/\mu_p G_D$ and G_{Ep}/G_D form factors. The solid lines denote fit I. The shadowed areas represent the 2σ (bright) and 3σ C.L. (dark) allowed regions. Kelly's fit [18] is shown by the dotted line.

for unpolarized *ep* elastic scattering reads (in the same notation used in the previous subsection):

$$\sigma(E,Q^2) \equiv \frac{d\sigma_{1\gamma}}{d\cos\theta} = \sigma_{\rm M}(E,Q^2)\left(G_{Ep}^2 + \frac{\tau}{\epsilon}\,G_{Mp}^2\right)\left(\frac{1}{1+\tau}\right), \tag{11}$$

$\sigma_{\rm M}$ being the Mott's differential cross section

$$\sigma_{\rm M}(E,Q^2) \equiv \left(\frac{d\sigma}{d\cos\theta}\right)_{\rm M} = \frac{\pi\alpha^2 E'\cos^2(\theta/2)}{2E^3\sin^4(\theta/2)}\,. \tag{12}$$

The Rosenbluth separation is then obtained by considering the reduced differential cross section

$$\sigma_{\rm R}(E,Q^2) \equiv \epsilon\,(1+\tau)\,\frac{\sigma(E,Q^2)}{\sigma_{\rm M}(E,Q^2)} = \tau\,G_{Mp}^2(Q^2) + \epsilon\,G_{Ep}^2(Q^2)\,. \tag{13}$$

A linear fit of the reduced differential cross section at fixed Q^2 and different values of ϵ gives the value of $\tau G_{Mp}^2(Q^2)$ from the intercept ($\epsilon = 0$) and the value of $G_{Ep}^2(Q^2)$ from the slope. Notice, however, that the measurement of $G_{Ep}^2(Q^2)$ with the Rosenbluth method has large uncertainties, because the contribution of $G_{Ep}^2(Q^2)$ to the reduced differential cross section in Eq. (13) is suppressed for large values of Q^2 ($\tau \gtrsim \epsilon$) while for small values of Q^2 we have $G_{Ep}^2 \simeq G_{Mp}^2/\mu_p \simeq G_{Mp}^2/7.8$.

In our analysis, in the first fit, later called *fit I*, we assume that G_{Ep} is related to G_{Mp} by the linear relation of Eq. (7), which is favored by the direct measurement of $\mathcal{R}(Q^2)$ in polarization experiments, as discussed in Section 2.1.

For the proton magnetic form factors we adopt the parameterization proposed by Kelly [18]:

$$\frac{G_{Mp}(Q^2)}{\mu_p} = \frac{1+\sum_{k=1}^{n} a_{p,k}^M \tau^k}{1+\sum_{k=1}^{n+2} b_{p,k}^M \tau^k}\,, \tag{14}$$

which guarantees the asymptotic behavior $G_{Mp}(Q^2) \propto Q^{-4}$ at high Q^2 [39]. We shall employ the parameterization of Eq. (14) with 4 parameters ($n = 1$):

$$\frac{G_{Mp}(Q^2)}{\mu_p} = \frac{1+a_{p,1}^M\tau}{1+b_{p,1}^M\tau + b_{p,2}^M\tau^2 + b_{p,3}^M\tau^3}\,. \tag{15}$$

We will see that this choice turns out to be quite satisfactory for the description of the data. Moreover a relatively small number of parameters allows a better control of the errors.

We have also performed a fit with both the magnetic and electric proton form factors parameterized by the expression (15). This fit will be called *fit II* in the following. In this case the electric form factor reads:

$$G_{Ep}(Q^2) = \frac{1 + a^E_{p,1}\tau}{1 + b^E_{p,1}\tau + b^E_{p,2}\tau^2 + b^E_{p,3}\tau^3}\,. \tag{16}$$

In our analysis we consider similar sets of cross section data as the ones employed by Arrington in Ref. [17], namely the data from Ref. [40]-[62]. Some of the data were taken from the JLab data base [63]; we include also data from Ref. [64]. Additionally, we considered the latest data of JLab experiment [10] in which the cross section was measured with the smallest errors, up to-date.

We fitted the *ep* cross section data by minimizing the least-squares function

$$\chi^2_{\rm cs} = \sum_{i=1}^{M_{\rm cs}} \left\{ \sum_{j=1}^{N_i^{\rm cs}} \frac{\left[n_i \sigma^{\rm exp}_{i,j} - \sigma(E_{i,j}, Q^2_{i,j})\right]^2}{(\Delta\sigma^{\rm exp}_{i,j})^2} + \frac{(1-n_i)^2}{(\Delta n_i)^2} \right\}, \tag{17}$$

where $M_{\rm cs} = 24$ or $M_{\rm cs} = 28$ [2] are the numbers of data sets, $N_i^{\rm cs}$ is the number of points in the ith data set, n_i and Δn_i are the corresponding overall normalization and uncertainty, $\sigma^{\rm exp}_{i,j}$ is the jth differential cross section point in the ith data set, with electron energy $E_{i,j}$ and four-momentum transfer $Q^2_{i,j}$, $\sigma(E_{i,j}, Q^2_{i,j})$ is the corresponding differential cross section computed with Eq. (11). The uncertainty $\Delta\sigma_{i,j}$ of $\sigma^{\rm exp}_{i,j}$ includes the statistical and uncorrelated systematic uncertainties added in quadrature.

We perform a *simultaneous* fit of the polarization and cross section data by minimizing the sum of the least-square functions, Eqs. (8) and (17):

$$\chi^2 = \chi^2_{\rm rat} + \chi^2_{\rm cs}\,. \tag{18}$$

For the fit I the range of Q^2 taken into account is

$$0.1\,{\rm GeV}^2 \le Q^2 \le 6\,{\rm GeV}^2\,, \tag{19}$$

which corresponds to the interval of Q^2 values where polarization transfer data are available.

For the fit II we extend the range of Q^2 down to $Q^2 \simeq 0$:

$$0 \le Q^2 \le 6\,{\rm GeV}^2\,. \tag{20}$$

Notice that a precise knowledge of the form factors in the low Q^2 region is of special interest for neutrino-nucleon (-nucleus) scattering processes. In both cases the upper limit, $Q^2 = 6$ GeV^2, is determined by the polarization data. We do not consider higher Q^2 points.

As already stressed in the literature [11], the inclusion of the most precise data of Ref. [10] definitely indicates the need of corrections to formula (11). Beyond the classical radiative corrections [65], to get agreement with the polarization data, one needs to consider also the two photon exchange (TPE) corrections, which can be written as an additive term to the reduced cross section:

$$\sigma_R \to \sigma_R + \delta_{TPE}. \tag{21}$$

The calculation of δ_{TPE} is difficult and model dependent: however, one can use general properties to derive a phenomenological expression of the TPE term. The scattering amplitude for electron-nucleon interaction must satisfy general symmetry properties, such as crossing symmetry and C-invariance [66]. They can be used to constrain δ_{TPE}.

Following Ref. [67] we adopt a TPE correction given by a function $F(Q^2, y)$

$$\sigma_R \to \sigma_R + \tau F(Q^2, y) \tag{22}$$

---

[2] For $Q^2 \in (0.1, 6)$ we have 24 independent data sets while for $Q^2 \in (0, 6)$ we have 28 independent data sets.

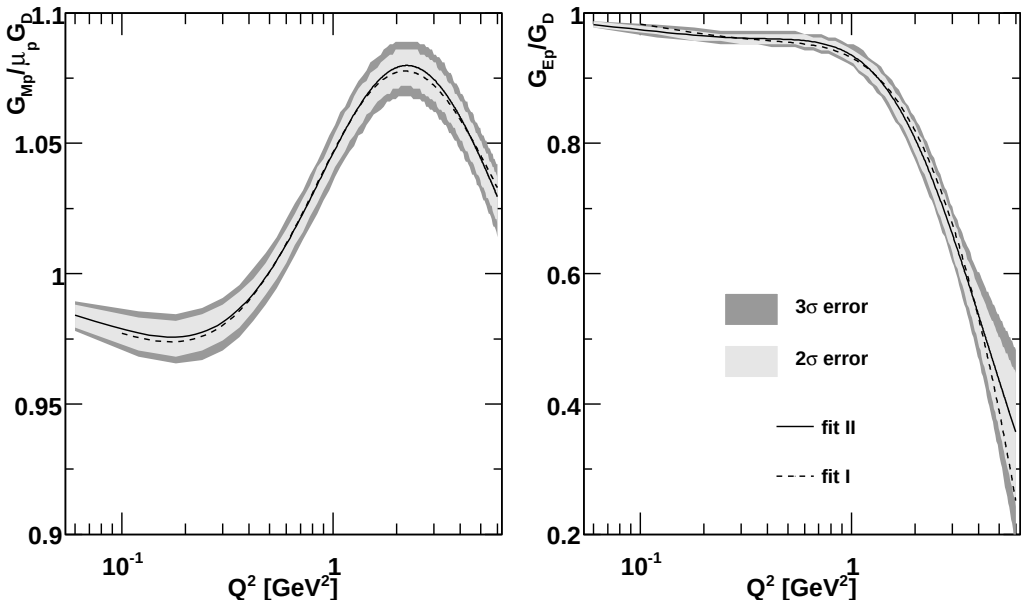

FIG. 4: Electric and magnetic proton form factors. The solid lines denote the best fit II. The shadowed areas represent the 2σ (bright) and 3σ C.L. (dark) allowed regions. Our previous fit I is shown with the dashed lines.

where

$$y = \sqrt{\frac{1-\epsilon}{1+\epsilon}}\,. \tag{23}$$

The function $F(Q^2, y)$ must satisfy the relation $F(Q^2, y) = -F(Q^2, -y)$. The analytical properties of $F(Q^2, y)$ allow one to express this function as a series of odd powers of y. Chen *et al.* [67] truncated the expansion to the second term:

$$F(Q^2, y) = \alpha G_D^2(Q^2) y + \beta G_D^2(Q^2) y^3, \tag{24}$$

α and β being fit parameter and $G_D(Q^2)$ the usual dipole form factor:

$$G_D(Q^2) = \left(1 + \frac{Q^2}{M_V^2}\right)^{-2}, \qquad \text{with} \qquad M_V^2 = 0.71\,\text{GeV}^2\,. \tag{25}$$

We consider both types of fit; for the fit I we obtained:

$$\chi^2_{\text{min}}/\text{NDF} = 375.97/392, \quad \text{GoF} = 71\%\,, \tag{26}$$

with the following values for the best fit parameters:

$$a^M_{p,1} = 1.53 \pm 0.01\,,\ b^M_{p,1} = 12.87 \pm 0.07\,,\ b^M_{p,2} = 29.16 \pm 0.25\,,\ b^M_{p,3} = 41.40 \pm 0.33\,,\ c_0 = 1.02 \pm 0.01\,,\ c_1 = -0.13 \pm 0.01\,. \tag{27}$$

The parameters of the TPE correction are:

$$\alpha = -0.39 \pm 0.09, \quad \beta = -0.04 \pm 0.09\,. \tag{28}$$

Notice that the values of c_0 and c_1 parameters are very similar to the ones in Eq. (9), obtained by fitting the polarization transfer data alone.

For the fit II the minimization procedure leads to:

$$\chi^2_{\text{min}}/\text{NDF} = 450.95/468, \quad \text{GoF} = 71\%\,, \tag{29}$$

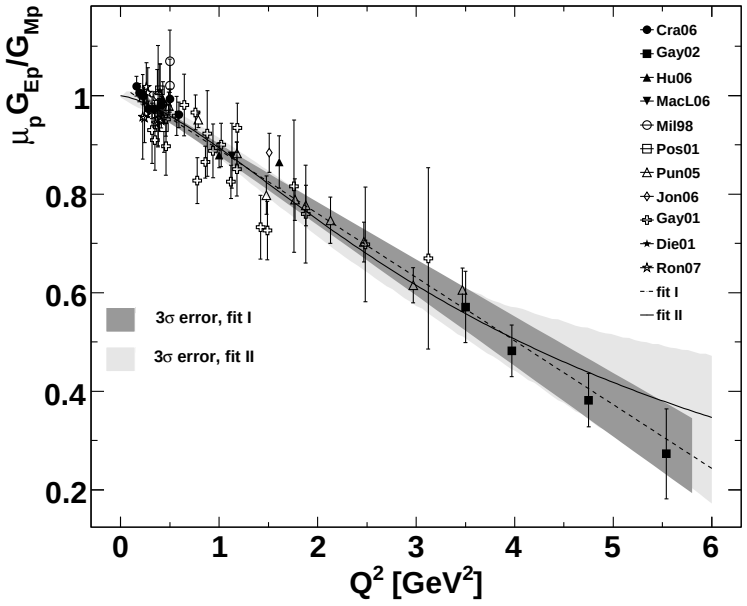

FIG. 5: The ratio $\mu_p G_{Ep}/G_{Mp}$ obtained in the simultaneous fit to polarization measurements and cross section data. fit I is shown by the dashed line, the corresponding 3σ C.L. allowed region being denoted by dark shadowed area. fit II is shown by the solid line, the corresponding 3σ C.L. allowed region being denoted by bright shadowed area.

with the following values for the fit parameters:

$$\begin{aligned} b^M_{p,1} &= 12.31 \pm 0.07\,,\ b^M_{p,2} = 25.57 \pm 0.22\,,\ b^M_{p,3} = 30.61 \pm 0.27, a^M_{p,1} = 1.09 \pm 0.01\,, \\ b^E_{p,1} &= 11.12 \pm 0.15\,,\ b^E_{p,2} = 15.16 \pm 1.03\,,\ b^E_{p,3} = 21.25 \pm 3.27\,,\ a^E_{p,1} = -0.19 \pm 0.06. \end{aligned} \tag{30}$$

The parameters of the TPE correction are:

$$\alpha = -0.36 \pm 0.09, \quad \beta = -0.08 \pm 0.09. \tag{31}$$

We remark that from both fits we obtained comparable values of the TPE parameters (see Fig. 2, which illustrates the allowed regions in the (α, β) parameter space with a given confidence level (C.L.)). In both cases the TPE correction turns out to be negative. Let us mention that the way we introduce the TPE corrections in our analysis also motivates the choice for the upper Q^2 limit: indeed, following the approach of Ref. [67], the magnitude of TPE is *fitted* to the data and, in the elastic cross section, it can be comparable to the magnitude of G_{Ep}. Hence the inclusion of the polarization data (which are less affected by TPE correction) allows a more precise determination of the TPE fit parameters, but restricts the Q^2 range to the one of the available polarization data.

It is worth mentioning that by excluding the TPE correction (hence using for the cross section formula (11)) both fits worsen, particularly in the goodness of fit. For the fit I we obtain $\chi^2_{\rm min}/{\rm NDF} = 467.07/394$ with GoF = 0.6%; similarly for the fit II we get $\chi^2_{\rm min}/{\rm NDF} = 544.31/470$ with GoF = 1%. We noticed that this result stems from the presence, in the analysis, of the very accurate JLab data [10], without which GoF would increase to 45% and 47%, respectively.

In addition to the above discussed form factors, we also checked a different parameterization, based on a two-poles formula for both the electric and magnetic proton form factors [5]:

$$G_{Ep}(Q^2) = \frac{a^E_1}{1 + a^E_2 Q^2} + \frac{1 - a^E_1}{1 + a^E_3 Q^2} \tag{32}$$

$$\frac{G_{Mp}(Q^2)}{\mu_p} = \frac{a^M_1}{1 + a^M_2 Q^2} + \frac{1 - a^M_1}{1 + a^M_3 Q^2}. \tag{33}$$

With respect to Kelly's parameterization this would offer the advantage of having a smaller number of parameters, in addition to the ones of the TPE correction. A new, global fit, can be obtained with $\chi^2_{\rm min}/{\rm NDF} = 1.10$ but GoF = 0.06%, thus indicating that the former parameterization is preferable.

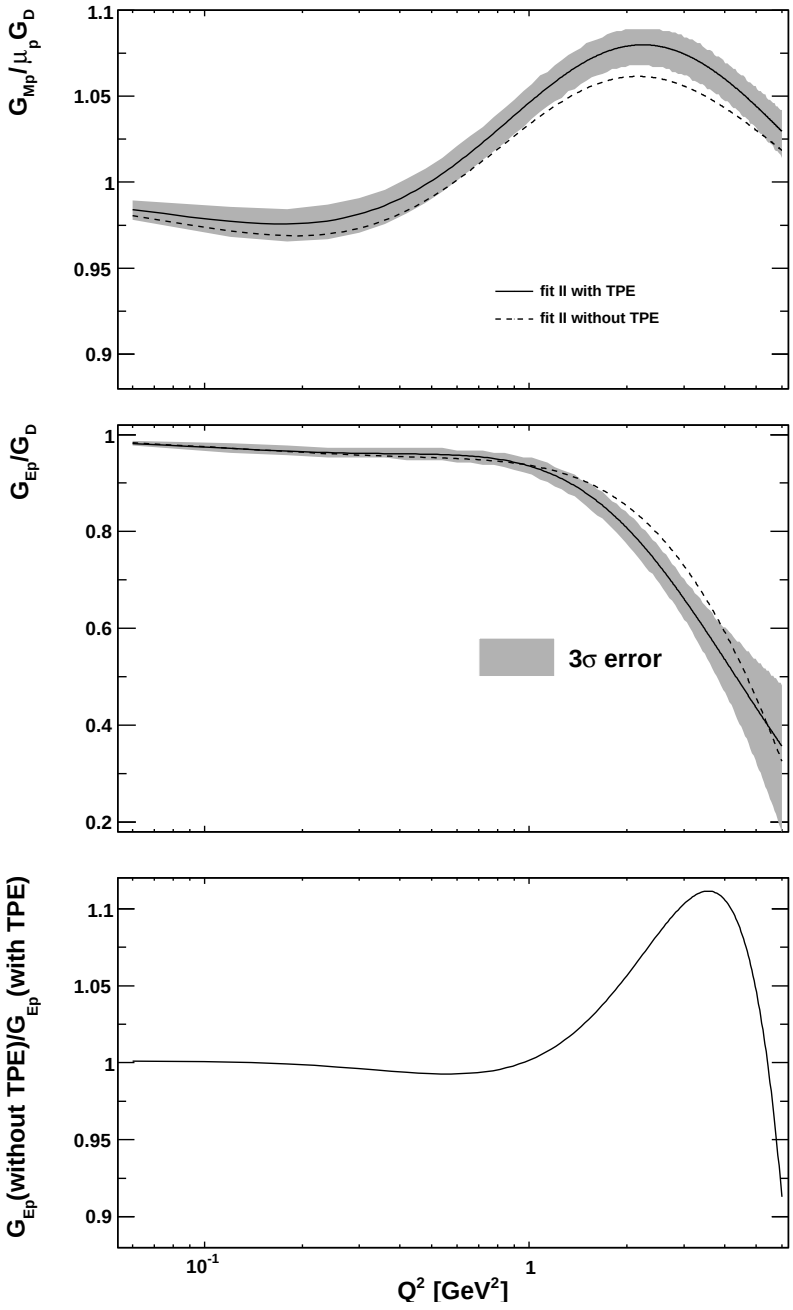

FIG. 6: Comparison of fits obtained with and without TPE correction (solid and dashed lines correspondingly). In the first and second panels $G_{Mp}/(\mu_p G_D)$ and G_{Ep}/G_D are plotted, respectively. The shadowed areas denote the 3σ. allowed regions. In the bottom panel the ratio (37) is shown. Results are obtained for fit II.

As it has been already mentioned in the introduction, one of our main tasks is to compute the form factor uncertainties as they can be extracted from the fit. This goal can be achieved by performing an accurate error analysis on the various fit parameters.

We calculated the correlated uncertainties of the fit parameters and the related uncertainties of the form factors with

the standard least-squares method, which is appropriate and widely used for non-linear models[3] (see Ref. [38, 68, 69]): the allowed region in the space of N parameters with λ confidence level (C.L.) is delimited by the contour defined by

$$\chi^2 = \chi^2_{\rm min} + \Delta\chi^2(N,\lambda)\,, \tag{34}$$

where $\Delta\chi^2(N,\lambda)$ is the value for which a χ^2 variable with N degrees of freedom has a cumulative probability λ. We consider 2σ (95.45% C.L.) and 3σ (99.73% C.L.) uncertainties.

Since we have 8 parameters in fit I and 10 parameters in fit II, the exploration of the parameter space in order to find the contours defined by Eq. (34) cannot be done with the simplest grid method. Therefore, we used a Monte Carlo Markov Chain generator of random points, which allows to find the allowed parameter regions with good accuracy in a few hours of CPU time of a normal PC.

It is interesting to notice, that the estimated values of the magnetic form factor parameters, $a^M_{p,1}$, $b^M_{p,1}$, $b^M_{p,2}$ and $b^M_{p,3}$ are strongly correlated. In particular, the estimates of a_1 and b_3 are almost linearly dependent. These parameters determine the asymptotic behavior of $G_{Mp}(Q^2)$, which turns out to be:

$$\lim_{Q^2\to\infty} Q^4 G_{Mp}(Q^2) = (4M^2)^2\,\frac{a^M_{p,1}}{b^M_{p,3}} \simeq (0.68\,^{+0.01}_{-0.01}\,{\rm GeV}^2)^2\,, \tag{35}$$

in fair agreement with the one given by the usual dipole form factor (25) (the above uncertainties are at 3σ).

In Fig. 2 (left panel) the error contours for α and β parameters are shown. Let us notice that solutions with β positive but very small are possible, but in this case α should be negative and large in magnitude. Therefore the TPE correction are always negative.

In Fig. 3 we show our best fits (fit I) for the magnetic and electric proton form factors with their uncertainties. We compare with Kelly's fit [18]. One can see that Kelly's fits of the magnetic proton form factor lies within our 3σ C.L. region in almost the whole Q^2 range under consideration. For the electric form factor the fits differ by more than 3σ in a relatively wide range of Q^2.

A similar error analysis is performed for fit II. Here, the number of form factor parameters is larger (4 parameters for each form factor). Similarly as above we show contour plot for the TPE correction parameters (Fig. 2, right panel).

Analogously to the case of fit I the estimates of the parameters $a^M_{p,1}$ and $b^M_{p,3}$ are linearly dependent and their ratio is similar:

$$\lim_{Q^2\to\infty} Q^4 G_{Mp}(Q^2) = (4M^2)^2\,\frac{a^M_{p,1}}{b^M_{p,3}} \simeq (0.66\,^{+0.02}_{-0.02}\,{\rm GeV}^2)^2. \tag{36}$$

One could also derive from the form factor parameters the charge and magnetic root-mean-square radii for the proton, as given by the slope of the electric and magnetic form factors at $Q^2 = 0$. They turn out to be: $\sqrt{< r^2_{Ep} >} = 0.87 \pm 0.01\,{\rm fm}$, $\sqrt{< r^2_{Mp} >} = 0.86 \pm 0.01$, fm. These results are comparable with previous analysis in the literature, but slightly lower than the most recent and advanced estimates of Ref. [70, 71]; indeed the latter take into account Coulomb distortion, which is relevant at low Q^2. For example Ref. [71] provides $\sqrt{< r^2_{Ep} >} = 0.895 \pm 0.018\,{\rm fm}$. The present fit of the form factors is carried out in plane-wave approximation and low-Q^2 properties like charge and magnetic radii are not properly reproduced without accounting for radiative corrections to the Rosenbluth cross sections.

In Fig. 4 we present G_{Mp} and G_{Ep} obtained in fit II, with the 2σ and 3σ C.L. error bands (represented by shadowed areas). Here the results from fit I are also plotted. Both fits lead to very similar magnetic form factors. On the contrary, there is a visible difference between the corresponding electric form factors: the G_{Ep} obtained in fit I decreases faster then the one obtained in fit II.

Fig. 5 shows the ratio $\mu_p G_{Ep}/G_{Mp}$ obtained with the fits I and II. The linear ratio fitted only to the polarization data is no longer shown, since it is very similar to the one obtained with fit I. The ratio uncertainties are larger for the fit II than for fit I due to the fact that the parameterization in fit II contains a larger number of degrees of freedom.

---

[3] In this case, the uncertainties of the parameters and their correlations estimated from the covariance matrix are quite approximate. This method was widely used in the past, when computer power was insufficient to perform more accurate evaluations, as the one presented in this paper.

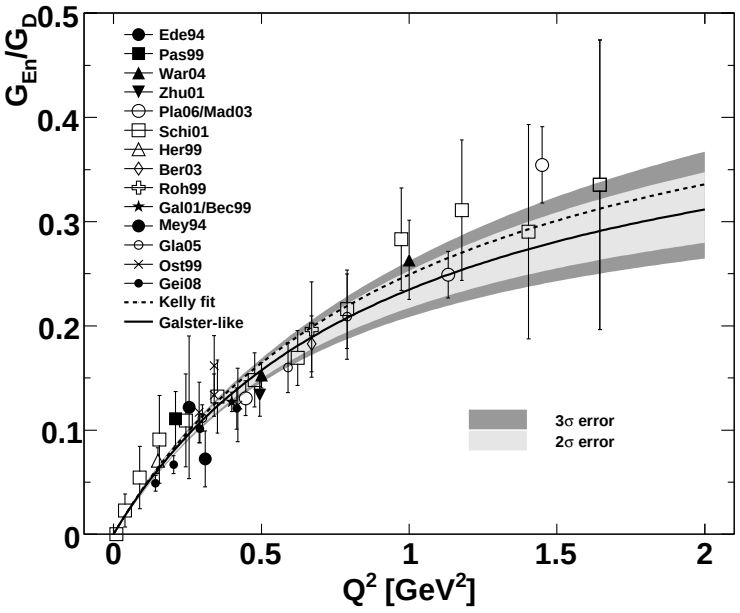

FIG. 7: Fit of the electric neutron form form factor (solid line). The Galster-like parameterization (38) is considered. The shadowed areas denote the 2σ (bright) and 3σ C.L. (dark) allowed regions. Kelly's fit [18] is shown with the dotted line.

Finally, given for granted that they are necessary, it is interesting to understand which is the *quantitative* impact of the TPE correction: they are expected to be relevant especially for the electric form factor. For this purpose we compare in Fig. 6 the proton form factors obtained with and without TPE correction – only fit II is considered. The magnetic proton form factor obtained without TPE is systematically shifted down by about 1.5%, and above $Q^2 \simeq 1$ GeV^2 it lies outside the 3σ C.L. region of the form factor obtained by including the TPE correction. The analogous effect on the electric form factor is shown in the middle panel of the same figure and appears to be less uniform than for the magnetic form factor: this can be better appreciated from the bottom panel of Fig. 6, where the ratio

$$G_{Ep}(\text{without TPE})/G_{Ep}(\text{with TPE}) \tag{37}$$

is plotted. One can see that the TPE correction substantially alters the Q^2 dependence of the electric form factor, in particular, for $Q^2 > 2$ GeV^2, with an effect which grows up to the order of 10%. In any case the impact of the TPE correction turns out to be non-negligible for both form factors.

3. NEUTRON FORM FACTORS

The measurement of the neutron form factors is much more difficult than that of the proton form factors, since a target of free neutrons does not exist. The neutron form factors are extracted from measurements of electron-nucleus scattering, usually electron-deuteron or electron-helium scattering. Therefore, the data analysis is affected by uncertainties stemming from the nuclear theoretical model assumed to describe the target nucleus. Since these models have consistently improved with time, in our analysis we consider only relatively recent data. At variance with the proton case, we take from the literature directly the published values of neutron form factors "data" and apply our fitting procedure to them.

3.1. Electric neutron form factor

For the electric neutron form factor we adopt the Galster-like parameterization

$$G_{En}(Q^2) = \frac{A\tau}{1 + B\tau}\, G_D(Q^2)\,, \tag{38}$$

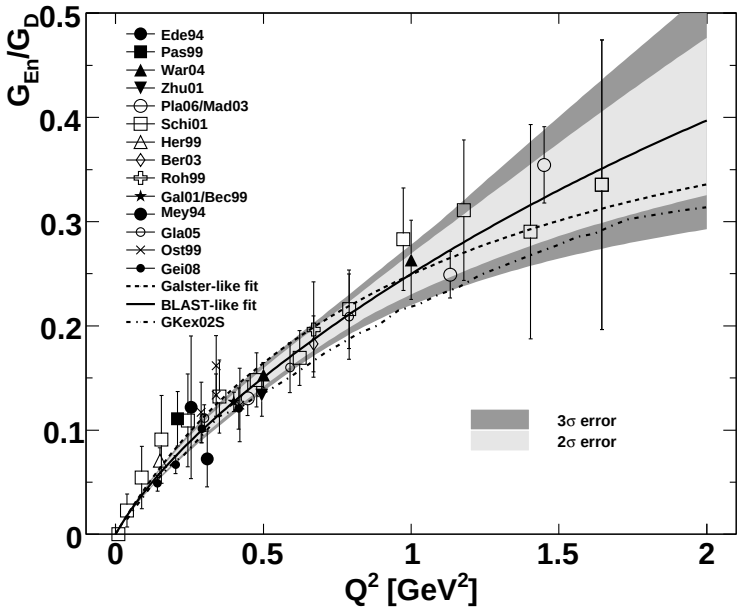

FIG. 8: Fit of the electric neutron form form factor (solid line). The BLAST-like parameterization (42) is shown. The shadowed areas represent the 2σ (bright) and 3σ C.L. (dark) allowed regions. The dashed line denotes the Galster-like parameterization. The Lomon result (GKex02S) [22] is denoted by the dash-dotted line.

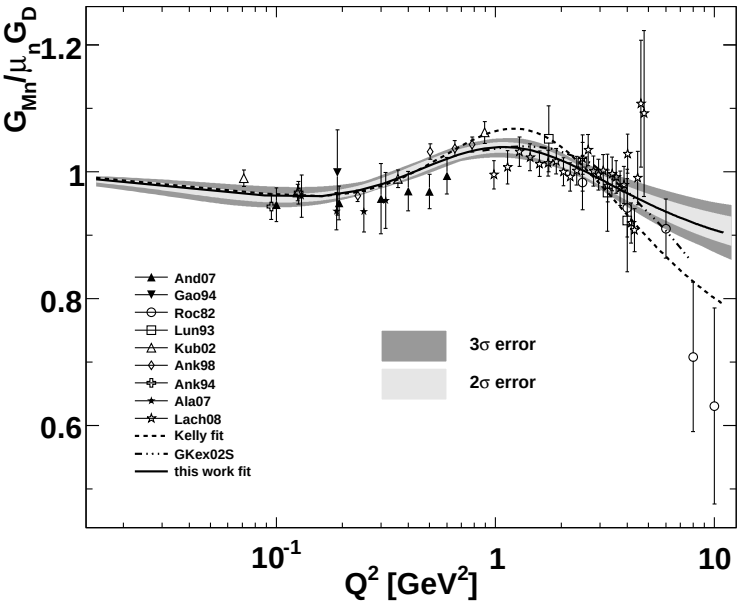

FIG. 9: Fit of magnetic neutron form factor (solid line), normalized to the dipole form factor. The shadowed areas denote 2σ (bright) and 3σ C.L. (dark) allowed regions. Kelly's fit [18] is shown with dotted line.

with the dipole form factor of Eq. (25).

We consider the electric neutron form factors "data" which have been published in several papers. Some of the data have been obtained in asymmetry and recoil polarization measurements [72, 73, 74, 75, 76, 77, 78, 79, 80, 81, 82, 83, 84, 85]. We consider also the reanalyzed electron-deuteron data [86] and the newest BLAST measurements [87]. Additionally, in order to have a proper slope of the electric form factor in the limit $Q^2 \to 0$, we impose to our fit the

additional constrain [88]:

$$\langle r_{En}^2 \rangle = -0.1148 \pm 0.0035 \text{ fm}^2. \tag{39}$$

We considered a least-squares function similar to the one in Eq. (8), with the experimental statistical and systematical uncertainties added in quadrature. With the values:

$$A = 1.68 \pm 0.05\,, \qquad B = 3.63 \pm 0.39\,, \tag{40}$$

we obtained

$$\chi^2_{\rm min}/{\rm NDF} = 25.82/37\,, \tag{41}$$

and the goodness of the fit turned out to be excellent: 91%.

In Fig. 7 we plot the best-fit value of G_{En} as a function of Q^2 together with the 2σ and 3σ C.L. allowed regions. We plot also Kelly's fit [18].

As an alternative to the most commonly used Galster-like parameterization, we considered a neutron electric form factor given by the sum of two dipole form factors:

$$G_{En}(Q^2) = \frac{a}{\left(1 + b_1 Q^2\right)^2} - \frac{a}{\left(1 + b_2 Q^2\right)^2}. \tag{42}$$

This parameterization is similar to the one considered in the latest BLAST data analysis [87] and for this reason we will call it BLAST-like parameterization. The fitting procedure for the above parameterization leads to:

$$\chi^2/NDF = 17.95/36, \quad \text{GoF} = 99\% \tag{43}$$

with the parameters:

$$a = -0.10 \pm 0.02, \quad b_1 = 2.83 \pm 0.37, \quad b_2 = 0.43 \pm 0.11. \tag{44}$$

In Fig. 8 the BLAST-like parameterization is compared to the data: the Galster-like parameterization and one of the recent Lomon parameterization [21, 22] (GKex02S) are also shown. Notice that the parameterization (44) raises faster with Q^2 than the Galster-like and the Lomon one, but the latter remain both within the BLAST parameterization uncertainties.

3.2. Magnetic neutron form factor

For the neutron magnetic form factor we adopted again the simplest form of Kelly's parameterizations, with $n = 1$:

$$\frac{G_{Mn}(Q^2)}{\mu_n} = \frac{1 + a_{n,1}^M \tau}{1 + b_{n,1}^M \tau + b_{n,2}^M \tau^2 + b_{n,3}^M \tau^3}\,. \tag{45}$$

We considered 11 data sets, obtained from asymmetry measurements [89]-[92], [93] and cross section measurements in electron-deuterium scattering [94]-[103], where Ref. [103] contains the latest JLab measurements. The fit to all these data sets leads, however, to a minimum $\chi^2/{\rm NDF} = 2.05$, not quite satisfactory. According to a remark of Kelly [70], the data from [101] and [97] were extracted using the same associated-particle technique for the neutron efficiency, a technique which appears to be in contradiction with the method used in other experiments. Therefore we omitted these two data sets. From our final analysis. After excluding the two above mentioned data sets, we obtained a fit over $N = 56$ points with

$$\chi^2_{min}/{\rm NDF} = 52.79/52 = 1.01, \tag{46}$$

and GoF = 44%. The corresponding values for the parameters in the neutron magnetic form factor are:

$$b_{n,1}^M \;=\; 21.30 \pm 4.56, \quad b_{n,2}^M = 77 \pm 31 \quad b_{n,3}^M = 238 \pm 105, \quad a_{n,1}^M = 8.28 \pm 3.89. \tag{47}$$

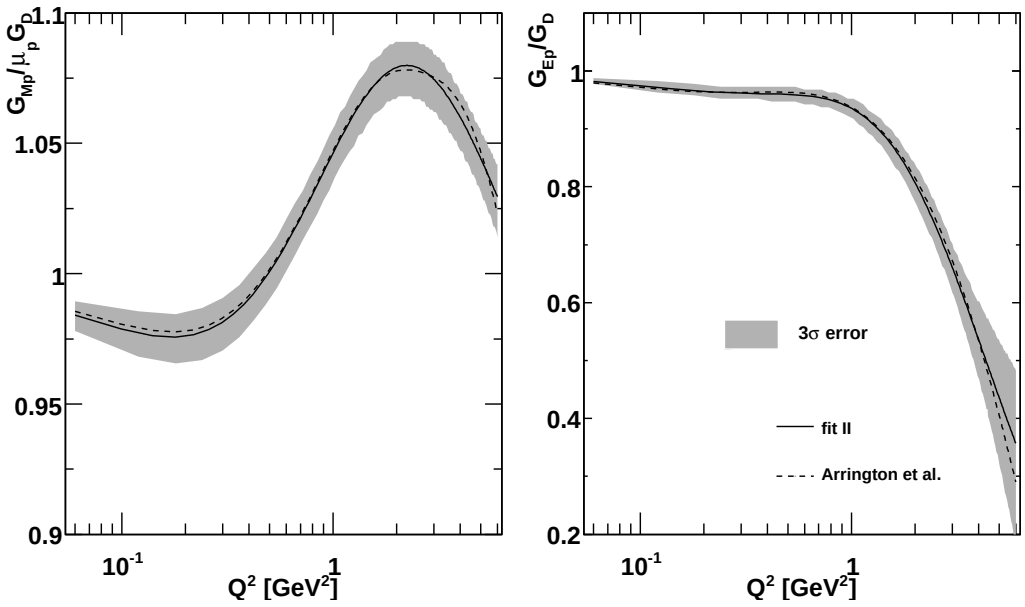

FIG. 10: Magnetic and electric proton form factors (normalized to the dipole form factor). The comparison between fit I (solid lines) and Arrington *et al.* [11] (dashed lines) is shown. The shadowed areas denote the 3σ C.L. allowed region.

We performed the error analysis over the four parameters above. Even if the fit of G_{Mn} was done on a slightly different basis than the one of the proton, yet we observe strong correlations between estimated values of the parameters, in full analogy with our findings for the proton form factor. In particular, the estimated values of parameters (a_1 and b_3) which determine the asymptotic behavior of the form factor at large Q^2 are almost linearly dependent:

$$\lim_{Q^2\to\infty} Q^4 G_{Mn}(Q^2) = (4M^2)^2 \frac{a^M_{n,1}}{b^M_{n,3}} \simeq (0.66^{+0.01}_{-0.01}\,\mathrm{GeV}^2)^2 \tag{48}$$

This value is very similar to the one obtained for the proton. Notice, however, that without the newest JLab data, instead of the value (48) we would get $(0.58^{+0.04}_{-0.05}\,\mathrm{GeV}^2)^2$. In Fig. 9 our final fit of G_{Mn} is different from Kelly's result [18] since it contains the newest JLab measurements.

4. DISCUSSION AND CONCLUSIONS

In this section we start by presenting further comparisons of the form factors resulting from our fits with the ones of previous data analyses.

In Ref. [11] the first systematical global analyses of the cross section and polarization transfer data on the proton with the inclusion of the TPE correction was performed. That fit is valid up to $Q^2 = 30$ GeV^2 for the magnetic form factor and up to 6 GeV^2 for the electric form factor. In Fig. 10 we display together our global fits and those of Ref. [11]: it clearly appears that, even thought different approaches for the TPE correction were employed, the global fits are very similar.

We also compare our fits with the recent one of Bodek *et al.* [20] (BBBA07). This global fit is tailored to accurately describe the form factors at low Q^2 as well as in the intermediate region of Q^2. These authors used the Kelly's parameterization with four parameters but each form factor was multiplied by some Legendre polynomial, which depends on several additional parameters, constrained to reproduce the low Q^2 behavior obtained in Ref. [19].

The authors of Ref. [20] plotted the form factors against the so-called Nachtman variable, which for the elastic scattering is defined as $\xi = 2/(1+\sqrt{1+1/\tau})$. Therefore in order to make the comparison with their results we express our form factors in terms of the ξ variable. Plots are shown in Fig. 11. In the region of ξ corresponding to the range of validity of our fits the predictions of the two parameterizations are very similar, however, our magnetic proton form factor is systematically higher (by several percent) then the one given by the BBBA07 parameterization.

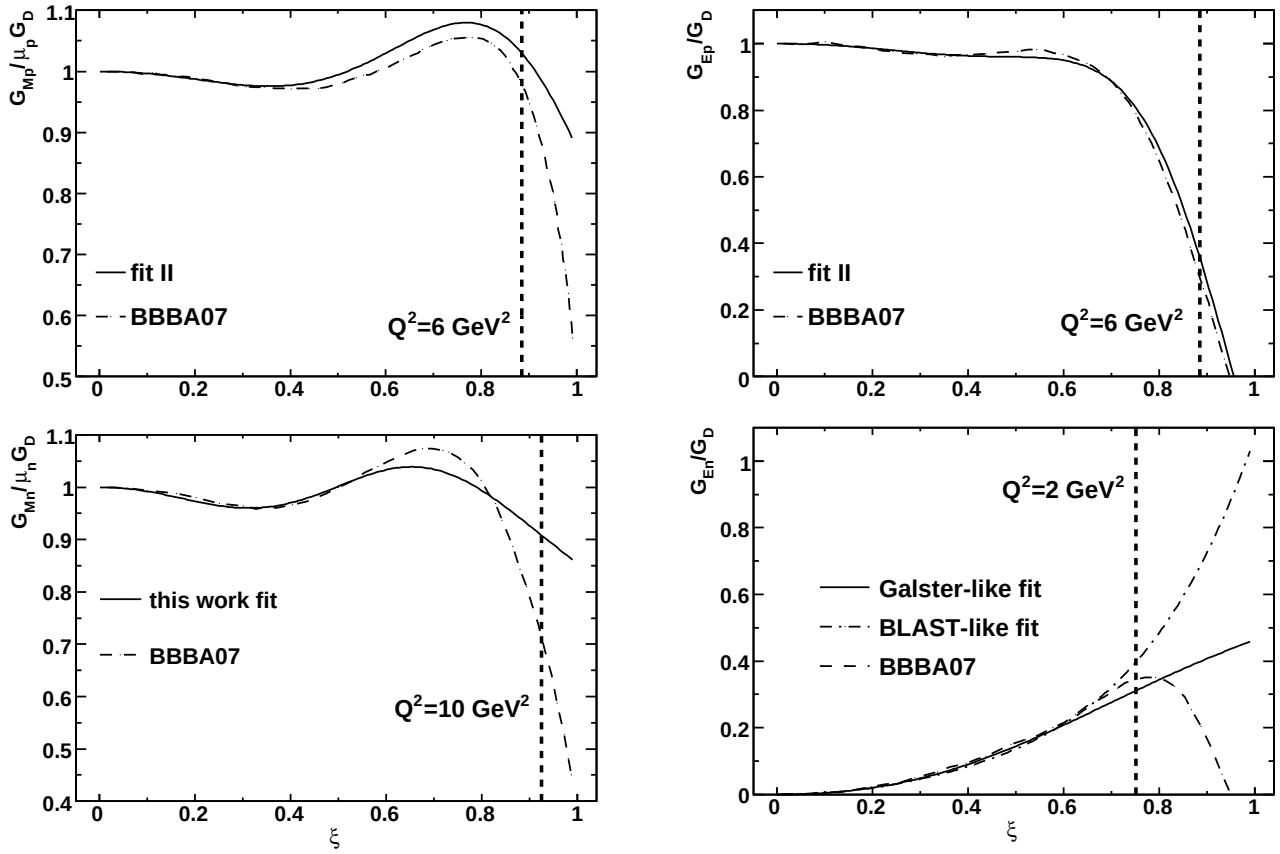

FIG. 11: Proton and neutron electric and magnetic form factors (normalized to the dipole form factor). The fits of electric and magnetic form factors (fit II) as well as the fit of neutron magnetic form factor are denoted by solid lines. BBBA07 [20] global fits are denoted by dashed lines. In the case of the electric neutron form factor, both parameterization, Galster and BLAST -like, are shown by the solid and dash-dotted lines, respectively. The form factors are plotted against the Nachtman variable. The dashed vertical bar represents the upper bound of the Q^2 range were our fits were performed.

The difference is given by TPE correction which we considered in our fitting procedure (see Fig. 6), while authors of Ref. [20] did not discuss this effect. For higher ξ values one can notice sizeable deviations for our form factors. However, we notice, that the ξ variable compresses in a very short range the large Q^2 region.

Finally we compare our estimates of uncertainties with those obtained by Arrington and Sick [19]: these authors did a serious attempt to compute the uncertainties of the nucleon form factors, which is a crucial information in the study of parity violating *ep* scattering. Their method to compute errors is explained in Ref. [19] and differs from our, in particular in the treatment of the systematic uncertainties. In particular we usually obtain asymmetric uncertainties around the best fit value: hence in Fig. 12 we compare the errors of Arrington and Sick on the electric and magnetic proton form factors with our lower and upper bounds for the 3σ confidence level errors. For the magnetic proton form factor, within the 3σ C.L. our results are consistent with the ones of Ref. [19]. For the electric proton form factor we notice some deviations between our results and the ones obtained by Arrington and Sick.

In conclusion we have presented two fits of the proton and neutron electromagnetic form factors, using the best available data. The *ep* elastic cross sections were reproduced by including a simple but realistic parameterization of the two photon exchange correction. Alternative parameterizations with fewer parameters than the one employed here do not allow to obtain equally good fits. We show that the impact of the TPE correction on the magnetic and electric proton form factors is larger than the 3σ uncertainty of the fits (in a wide range of Q^2). In fit I we constrained the electric proton form factor by the ratio $\mu_p G_{Ep}/G_{Mp}$ extracted from recoil polarization and asymmetry data. fit II employs Kelly's parameterization with four parameters both for the electric and magnetic proton form factors. This fit is obtained with two additional parameters with respect to fit I, however we believe that it is more reliable than

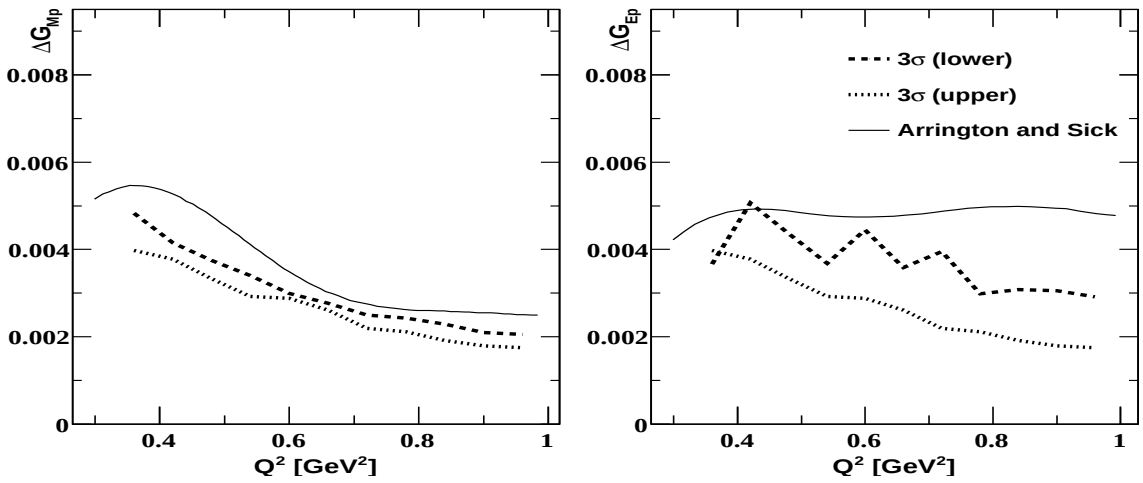

FIG. 12: The uncertainties of electric and magnetic proton form factors. Our computations (fit II) are denoted by dotted (upper uncertainties) and dashed lines (lower uncertainties) for the 3σ C.L. errors. The solid lines correspond to the results obtained in Ref. [19].

the former, particularly in the low Q^2 region. We also performed a careful analysis of the uncertainties resulting on the parameters of the fit and hence on the form factors. It is worth stressing that only a few papers, among the many devoted to the nucleon electromagnetic form factors, include the TPE correction in the analysis. As a final remark we remind the reader that even small uncertainties in the magnetic form factors of the proton and neutron turn out to be important for a correct analysis of the neutrino-nucleon cross sections.

The numerical results of our fits are available in the web site [37].

Acknowledgements

The authors acknowledge fruitful discussions with E. L. Lomon and T. W. Donnelly. K. M. G. thanks Ron Gilman for his remarks on the previous version of the manuscript, which helped to improve the present one.

S. M. B. has been supported by funds of the Munich Cluster of Excellence (Origin and Structure of the Universe), the DFG (Transregio 27: Neutrinos and Beyond) and by INFN Sezione di Torino.

K. M. G. was supported by WWS project founds.

[1] H. y. Gao, Int. J. Mod. Phys. E **12** (2003) 1 [Erratum-ibid. E **12** (2003) 567].
[2] J. Arrington, C. D. Roberts and J. M. Zanotti, J. Phys. G **34** (2007) S23.
[3] C. F. Perdrisat, V. Punjabi and M. Vanderhaeghen, Prog. Part. Nucl. Phys. **59** (2007) 694.
[4] R. Gran *et al.* [K2K Collaboration], Phys. Rev. D **74** (2006) 052002.
[5] W. M. Alberico, S. M. Bilenky, C. Giunti and C. Maieron, Z. Phys. C **70** (1996) 463.
[6] P. A. M. Guichon and M. Vanderhaeghen, Phys. Rev. Lett. **91** (2003) 142303.
[7] P. G. Blunden, W. Melnitchouk and J. A. Tjon, Phys. Rev. Lett. **91** (2003) 142304.
[8] Y. C. Chen, A. Afanasev, S. J. Brodsky, C. E. Carlson and M. Vanderhaeghen, Phys. Rev. Lett. **93** (2004) 122301.
[9] A. V. Afanasev, S. J. Brodsky, C. E. Carlson, Y. C. Chen and M. Vanderhaeghen, Phys. Rev. D **72** (2005) 013008.
[10] I. A. Qattan *et al.*, Phys. Rev. Lett. **94** (2005) 142301.
[11] J. Arrington, W. Melnitchouk and J. A. Tjon, Phys. Rev. C **76** (2007) 035205.
[12] C. E. Carlson and M. Vanderhaeghen, Ann. Rev. Nucl. Part. Sci. **57** (2007) 171.
[13] P. E. Bosted, Phys. Rev. C **51** (1995) 409.
[14] E. J. Brash, A. Kozlov, S. Li and G. M. Huber, Phys. Rev. C **65** (2002) 051001.
[15] H. Budd, A. Bodek and J. Arrington, *Modeling quasi-elastic form factors for electron and neutrino scattering*, Presented at 2nd International Workshop on Neutrino - Nucleus Interactions in the Few GeV Region (NUINT 02), Irvine, California, 12-15 Dec 2002. arXiv:hep-ex/0308005.

[16] J. Arrington, Phys. Rev. C **68** (2003) 034325.
[17] J. Arrington, Phys. Rev. C **69** (2004) 032201.
[18] J. J. Kelly, Phys. Rev. C **70** (2004) 068202.
[19] J. Arrington and I. Sick, Phys. Rev. C **76** (2007) 035201.
[20] A. Bodek, S. Avvakumov, R. Bradford and H. Budd, Eur. Phys. J. C **53** (2008) 349.
[21] E. L. Lomon, Phys. Rev. C **64** (2001) 035204.
[22] E. L. Lomon, *Effect of revised R(n) measurements on extended Gari-Kruempelmann model fits to nucleon electromagnetic form factors*, arXiv:nucl-th/0609020.
[23] S. Galster, H. Klein, J. Moritz, K. H. Schmidt, D. Wegener and J. Bleckwenn, Nucl. Phys. B **32** (1971) 221.
[24] A. F. Krutov and V. E. Troitsky, Eur. Phys. J. A **16** (2003) 285.
[25] B. D. Milbrath *et al.* [Bates FPP collaboration], Phys. Rev. Lett. **80** (1998) 452 [Erratum-ibid. **82** (1999) 2221].
[26] M. K. Jones *et al.* [Jefferson Lab Hall A Collaboration], Phys. Rev. Lett. **84** (2000) 1398.
[27] S. Dieterich *et al.*, Phys. Lett. B **500** (2001) 47.
[28] T. Pospischil *et al.* [A1 Collaboration], Eur. Phys. J. A **12** (2001) 125.
[29] O. Gayou *et al.*, Phys. Rev. C **64** (2001) 038202.
[30] O. Gayou *et al.* [Jefferson Lab Hall A Collaboration], Phys. Rev. Lett. **88** (2002) 092301.
[31] V. Punjabi *et al.*, Phys. Rev. C **71** (2005) 055202 [Erratum-ibid. C **71** (2005) 069902].
[32] C. B. Crawford *et al.*, Phys. Rev. Lett. **98** (2007) 052301.
[33] B. Hu *et al.*, Phys. Rev. C **73** (2006) 064004.
[34] M. K. Jones *et al.* [Resonance Spin Structure Collaboration], Phys. Rev. C **74** (2006) 035201.
[35] G. MacLachlan *et al.*, Nucl. Phys. A **764** (2006) 261.
[36] G. Ron *et al.*, Phys. Rev. Lett. **99** (2007) 202002.
[37] http://www.nu.to.infn.it/pap/08/ff/ff.php.
[38] C. Amsler *et al.* [Particle Data Group], Phys. Lett. B **667** (2008) 1.
[39] S. J. Brodsky and G. R. Farrar, Phys. Rev. Lett. **31** (1973) 1153.
[40] T. Janssens, R. Hofstadter, E. B. Hughes and M. R. Yearian, Phys. Rev. **142** (1966) 922.
[41] W. Bartel *et al.*, Phys. Rev. Lett. 17, 608 (1966).
[42] W. Albrecht, H. J. Behrend, F. W. Brasse, W. Flauger, H. Hultschig and K. G. Steffen, Phys. Rev. Lett. **17** (1966) 1192.
[43] W. Albrecht, H. J. Behrend, H. Dorner, W. Flauger and H. Hultschig, Phys. Rev. Lett. **18** (1967) 1014.
[44] J. Litt *et al.*, Phys. Lett. B **31** (1970) 40.
[45] M. Goitein *et al.*, Phys. Rev. D **1** (1970) 2449.
[46] L. E. Price, J. R. Dunning, M. Goitein, K. Hanson, T. Kirk and R. Wilson, Phys. Rev. D **4** (1971) 45.
[47] C. Berger, V. Burkert, G. Knop, B. Langenbeck and K. Rith, Phys. Lett. B **35** (1971) 87.
[48] F. Borkowski, P. Peuser, G. G. Simon, V. H. Walther and R. D. Wendling, Nucl. Phys. A **222** (1974) 269.
[49] P. N. Kirk *et al.*, Phys. Rev. D **8** (1973) 63.
[50] W. Bartel *et al.*, Nucl. Phys. B **58** (1973) 429.
[51] F. Borkowski, P. Peuser, G. G. Simon, V. H. Walther and R. D. Wendling, Nucl. Phys. B **93** (1975) 461.
[52] J. J. Murphy, Y. M. Shin and D. M. Skopik, Phys. Rev. C **9** (1974) 2125 [Erratum-ibid. C **10** (1974) 2111].
[53] S. Stein *et al.*, Phys. Rev. D **12** (1975) 1884.
[54] G. G. Simon, C. Schmitt, F. Borkowski and V. H. Walther, Nucl. Phys. A **333** (1980) 381.
[55] G. G. Simon, C. Schmitt and V. H. Walther, Nucl. Phys. A **364** (1981) 285.
[56] S. Rock *et al.*, Phys. Rev. D **46** (1992) 24.
[57] A. F. Sill *et al.*, Phys. Rev. D **48** (1993) 29.
[58] R. C. Walker *et al.*, Phys. Rev. D **49** (1994) 5671.
[59] L. Andivahis *et al.*, Phys. Rev. D **50** (1994) 5491.
[60] D. Dutta *et al.* [JLab E91013 Collaboration], Phys. Rev. C **68** (2003) 064603.
[61] M. E. Christy *et al.* [E94110 Collaboration], Phys. Rev. C **70** (2004) 015206.
[62] I. Niculescu, Ph.D. thesis, Hamptom University, 1999.
[63] http://www.jlab.org/resdata.
[64] R. G. Arnold *et al.*, Phys. Rev. Lett. **57** (1986) 174.
[65] L. W. Mo and Y. S. Tsai, Rev. Mod. Phys. **41** (1969) 205.
[66] M. P. Rekalo and E. Tomasi-Gustafsson, Eur. Phys. J. A **22** (2004) 331.
[67] Y. C. Chen, C. W. Kao and S. N. Yang, Phys. Lett. B **652** (2007) 269.
[68] D. E. Groom *et al.* [Particle Data Group], Eur. Phys. J. C **15** (2000) 1.
[69] W.T. Eadie, D. Drijard, F.E. James, M. Roos and B. Sadoulet, *Statistical Methods in Experimental Physics*, North Holland, 1971.
[70] J. J. Kelly, Phys. Rev. C **66** (2002) 065203.
[71] I. Sick, Phys. Lett. B **576** (2003) 62
[72] J. Bermuth *et al.*, Phys. Lett. B **564** (2003) 199.
[73] J. Golak, G. Ziemer, H. Kamada, H. Witala and W. Gloeckle, Phys. Rev. C **63** (2001) 034006.
[74] J. Becker *et al.*, Eur. Phys. J. A **6** (1999) 329.
[75] M. Meyerhoff *et al.*, Phys. Lett. B **327** (1994) 201.
[76] D. Rohe *et al.*, Phys. Rev. Lett. **83** (1999) 4257.
[77] H. Zhu *et al.* [E93026 Collaboration], Phys. Rev. Lett. **87** (2001) 081801.

[78] T. Eden *et al.*, Phys. Rev. C **50** (1994) 1749.
[79] C. Herberg *et al.*, Eur. Phys. J. A **5** (1999) 131.
[80] R. Madey *et al.* [E93-038 Collaboration], Phys. Rev. Lett. **91** (2003) 122002.
[81] I. Passchier *et al.*, Phys. Rev. Lett. **82** (1999) 4988.
[82] G. Warren *et al.* [Jefferson Lab E93-026 Collaboration], Phys. Rev. Lett. **92** (2004) 042301.
[83] D. I. Glazier *et al.*, Eur. Phys. J. A **24** (2005) 101.
[84] M. Ostrick *et al.*, Phys. Rev. Lett. **83** (1999) 276.
[85] B. Plaster *et al.* [Jefferson Laboratory E93-038 Collaboration], Phys. Rev. C **73**, 025205 (2006).
[86] R. Schiavilla and I. Sick, Phys. Rev. C **64** (2001) 041002.
[87] E. Geis *et al.* [BLAST Collaboration], Phys. Rev. Lett. **101** (2008) 042501.
[88] S. Kopecky, P. Riehs, J. A. Harvey and N. W. Hill, Phys. Rev. Lett. **74** (1995) 2427.
[89] B. Anderson *et al.* [Jefferson Lab E95-001 Collaboration], Phys. Rev. C **75** (2007) 034003.
[90] W. Xu *et al.*, Phys. Rev. Lett. **85** (2000) 2900.
[91] W. Xu *et al.* [Jefferson Lab E95-001 Collaboration], Phys. Rev. C **67** (2003) 012201.
[92] H. Gao *et al.*, Phys. Rev. C **50** (1994) 546.
[93] R. Alarcon [BLAST Collaboration], Eur. Phys. J. A **31** (2007) 588 [Eur. Phys. J. A **32** (2007) 477].
[94] H. Anklin *et al.*, Phys. Lett. B **336** (1994) 313.
[95] H. Anklin *et al.*, Phys. Lett. B **428** (1998) 248.
[96] W. K. Brooks and J. D. Lachniet [CLAS Collaboration], Nucl. Phys. A **755** (2005) 261.
[97] E. E. W. Bruins *et al.*, Phys. Rev. Lett. **75**, 21 (1995).
[98] E. E. W. Bruins *et al.*, Phys. Rev. Lett. **79** (1997) 5187.
[99] G. Kubon *et al.*, Phys. Lett. B **524**, 26 (2002).
[100] A. Lung *et al.*, Phys. Rev. Lett. **70** (1993) 718.
[101] P. Markowitz *et al.*, Phys. Rev. C **48** (1993) 5.
[102] S. Rock *et al.*, Phys. Rev. Lett. **49** (1982) 1139.
[103] J. Lachniet *et al.* [CLAS Collaboration], arXiv:0811.1716 [nucl-ex].